Investigation of anti-ablation property of C_f/HfC composite prepared at 1900℃ by reactive melt infiltration

Y.C. Ye *, H. Zhang, Y.G. Tong, L.A. Zhu, S.X. Bai, K. Chen

College of Aerospace and Materials Engineering, National University of Defense Technology, Changsha, 410073, PR China
**Yeyicong@gmail.com*

Keywords: C_f/HfC composite, ablation property, reactive melt infiltration.

Abstract

A quarternary Hf alloy (50Hf10Zr40Si3Ta) has been prepared and infiltrated into a C-C preform at 1900℃, much lower than the alloy melting point, to obtain the C_f/HfC composite, whose linear ablation rate by laser has been tested to be only 8×10^{-3} mm/s. The composite exhibits excellent oxidation-resistant and ablation-resistant properties because of the behavior of various oxides formed during the ablation by laser. First, a large amount of heat was taken away with the melt and evaporation of SiO_2, HfO_2, ZrO_2 and Ta_2O_5. Second, HfO_2, ZrO_2 and Ta_2O_5 in liquid state at the ablated temperature flew and sealed the cracks and holes in the composite. Last, a Ta_2O_5•$mHfO_2$ melt with a low vapor pressure and high viscosity was formed, which would block the diffusion of the oxygen to the inner of the composite.

1 Introduction

In recent years, carbon fiber reinforced UHTCs-based composites (C_f/UHTCs) have been widely studied due to their high mechanical performance and excellent anti-ablation property [1-4]. Of different kinds of C_f/UHTCs, the carbon fiber reinforced HfC-based composites (C_f/HfC) has attracted people's attention due to the very high melting point of HfC and its anti-ablation property [5].

Because of the short preparation period and low cost, reactive melt infiltration (RMI) has been a preferred method for preparing C_f/UHTCs [6-8]. However, it is unfeasible to prepare C_f/HfC by RMI because the melting point of pure hafnium is as high as 2230℃ and at this temperature the mechanical property of C/C composite will be weakened.

Still, basing on alloy design, our research group prepared the C_f/HfC composite by RMI at a relative low temperature below the alloy melting point, 1900℃. It is suggested that the primary reason for triggering the RMI process at a relative low temperature is that the Hf component with the most strong carbide-forming ability prefers to react with the carbon in the surface layer of the C-C preform, leading to a phase composition change of the alloy at the interface, generating liquid phase and forming a specific multi-layer RMI structure [9]. This paper is to discuss the anti-ablation property of the obtained C_f/HfC composite.

2 Experimental

2.1 Preparation of Cf/HfC composite

A 50Hf10Zr37Si3Ta alloy ingot was prepared in a vacuum arc furnace with pure hafnium (purity≥99.4%), zirconium (purity≥99.9%) and silicon (purity≥99.8%). PAN-based carbon fiber (T300, Toray, Japan) needled felts preforms were used as reinforcements, initial density of which is 1.28g/cm^3. The needled felts were prepared by the three-dimensional needling technique, starting with repeatedly overlapping the layers of 0°non-woven fiber cloth, short-cut-fiber web, and 90°non-woven fiber cloth with needle-punching step by step. Pyrolytic carbon (PyC) was then deposited on the surface of the carbon fibers by chemical vapor infiltration process.

The carbon/carbon preform (C/C preform) and the alloy ingot were put into a graphite crucible, which was then placed in a carbon tube furnace and heated up to 1900℃, holding for 30mins, followed by furnace cooling. RMI process took place in the meanwhile.

2.2 Ablation test

Ablative resistance properties were tested by a pulsed laser. A long pulse re-frequency Nd:YAG solid-state laser with the wave length of 1064nm and frequency of 1~500Hz was applied. The laser power of 1000 W was selected to vertically irradiate on the materials exposed in the air. The peak value of the laser power and the duty ratio was controlled by adjusting the pulse current, frequency and pulse width. The peak value of the laser power, repeat frequency, pulse width and average power are shown in Fig. 1.

Peak power was calculated by the following equation, in which the average power was measured by laser power meter and the duty ratio equals to pulse width times repeated frequency.

$$\text{Peak power} = \text{Average power} / \text{duty ratio}$$

Spot size was adjusted by changing the distance between the sample and focusing mirror. Power density is defined by the following equation.

$$\text{Power density} = \text{Power} / \text{facula area}$$

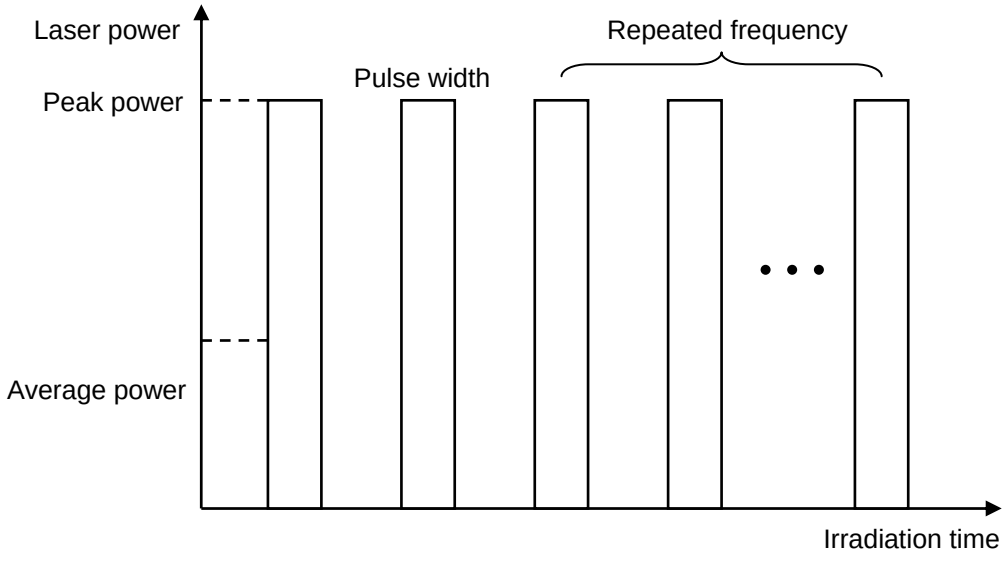

Figure 1. Parameters of repeated frequency laser irradiation

3 Results and discussion

3.1 Preparation and structure of the RMI sample

According to the previous research [9], it is decided that the elements of the designed alloy includes Hf, Zr, Si and Ta with a mole ratio of 50:10:37:3. The Hf content is not less than 50 at.% because the C_f/HfC composite is expected to be applied in very high temperature environment. The silicon and tantalum content should not be too high, because SiO_2 and Ta_2O_5 evaporate at very high temperature, which will do harm to the anti-ablation property of the composite. Zirconium is added into the alloy in order to decrease the melting point of the alloy and reduce the alloy density.

The cross section of the RMI sample was observed under SEM (Fig.2 a). The fracture micrograph (Fig.2 b) shows an obvious characteristic of the RMI structure, i.e., there are layers surrounding the carbon fibers. It is suggested that the white particles and grains are either HfC or ZrC, and the dark substance is SiC.

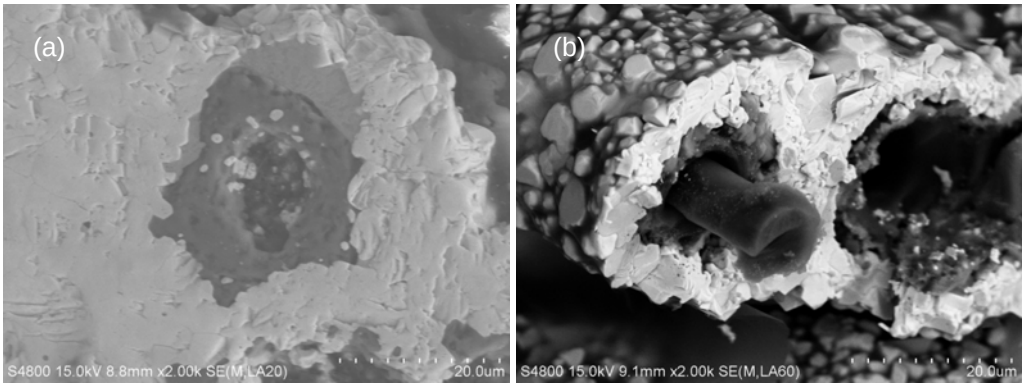

Figure 2. The cross section (a) and fracture micrograph (b) of the RMI sample under SEM.

3.2 Ablation properties of the RMI sample

The sample was tested by the laser with power of 1000 W/cm^2 for 60 s. Fig. 3 shows the surface morphology of the tested sample. A white protection layer formed in the ablation spot. It is seen from the micro-morphology (Region A and Region B) that the protection layer is very dense and compact without any obvious defects. Region A is nearer to the center of ablation spot. The typical morphology of Region A (Fig. 3 c) is different from that of Region B(Fig. 3 d). The grains in Region A are seemed to be larger and filiform chrysanthemum flower-like. The grains in Region B are smaller, inside which the microstructure is of decussation-like with white materials surrounding the dark gray skeleton in the center. The grains closely and continuously pack with each other, the size of which gradually decrease from the center of the ablation spot to the edge part. The EDS analysis result of Region A and B shows that the white protection layer is composed of Hf, Ta and O (Fig. 4).

The obtained composite is composed of HfC, ZrC, SiC, C and minor TaC phase, whose evolution during ablation is shown as the reaction equations in Table 1. SiO_2, HfO_2, ZrO_2 and Ta_2O_5 generate from the oxidation of HfC, ZrC, SiC and minor TaC.

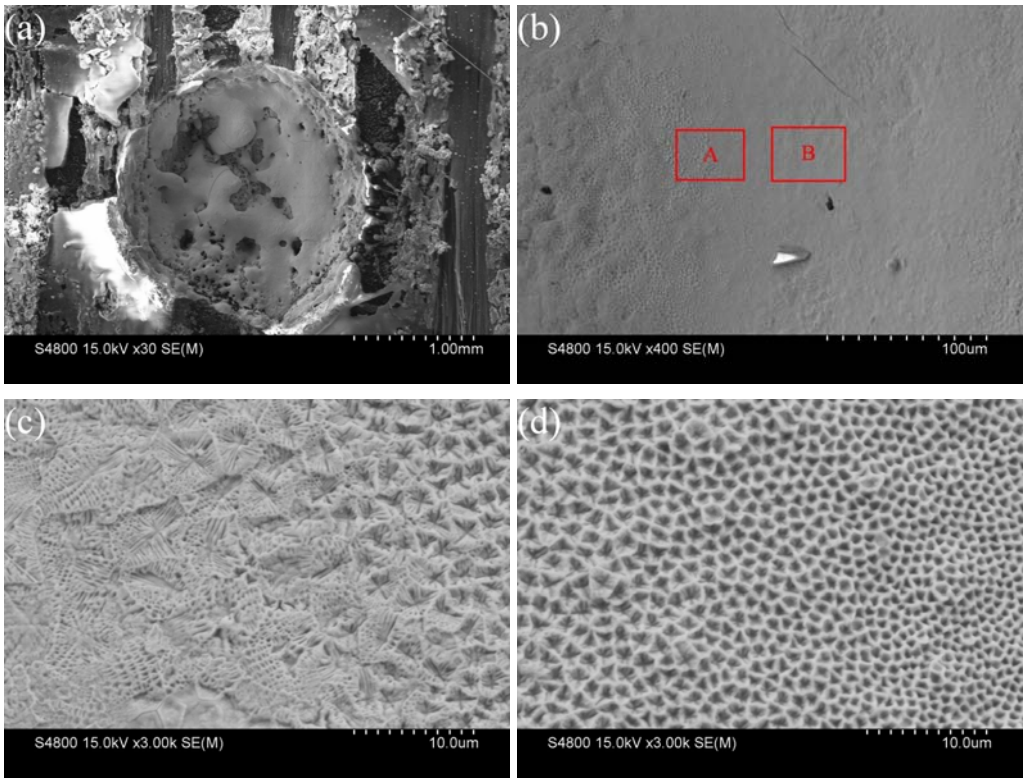

Figure 3. Ablation spot on the surface of the RMI sample (a) and Region A is nearer to the center of ablation spot while Region B is nearer to the edge (b). Region A (c) has a more coarsened microstructure than Region B (d) does.

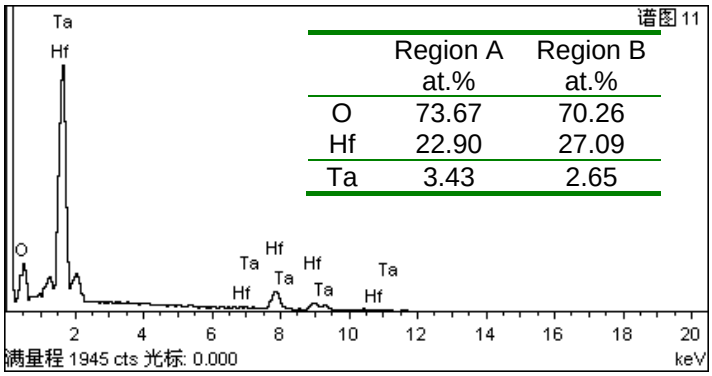

	Region A at.%	Region B at.%
O	73.67	70.26
Hf	22.90	27.09
Ta	3.43	2.65

Figure 4. EDS analysis results of Region A and B are similar. The Ta content is a little higher and the Hf content is a little lower in Region A than in Region B.

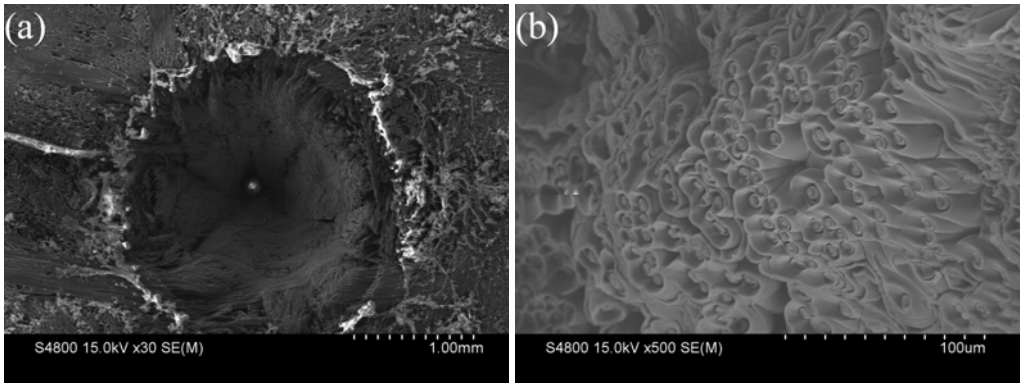

Figure 5. Ablation spot of C/C preform. (a) low magnification, (b) high magnification

No.	Reaction equations
1	$HfC(s) +3/2O_2(g)= HfO_2(s) +CO(g)$
2	$HfO_2(s)=HfO_2(l)$
3	$HfO_2(l)= HfO_2(g)$
4	$ZrC(s) +3/2O_2(g)=ZrO_2(s) +CO(g)$
5	$ZrO_2(s)=ZrO_2(l)$
6	$ZrO_2(l)=ZrO_2(g)$
7	$C(s)+1/2O_2(g)=CO(g)$
8	$CO(g)+1/2O_2(g)=CO_2(g)$
9	$SiC(s) +3/2O_2(g)=SiO_2(s) +CO(g)$
10	$SiO_2(s)=SiO_2(l)$
11	$SiO_2(l)=SiO_2(g)$
12	$TaC(s) +5/2O_2(g)= Ta_2O_5(s) +CO(g)$
13	$Ta_2O_5(s)= Ta_2O_5(l)$
14	$Ta_2O_5 (l)= Ta_2O_5 (g)$

Table 1. Possible reactions during the ablation process of the C_f/HfC composite

The temperature of the spot area rapidly increased to around 3000℃ when the laser power is 1000 W/cm^2, thus the SiO_2 phase immediately gasified without any trace cause the boiling point of SiO_2 is 2230℃. HfO_2 and Ta_2O_5 generated at high temperature as Reaction 1 and 12 shows, which formed mutual soluble melt around 3000℃ according to the HfO_2-Ta_2O_5 and ZrO_2-Ta_2O_5 phase diagram. The melt of high viscosity spread out on the surface of the sample and protected it from ablation. As the laser ablation finished, the melt solidified and $Ta_2O_5 \cdot m HfO_2$ phase generated. Therefore, the white protection layer is suggested to be $Ta_2O_5 \cdot m HfO_2$, the *m* value of which is higher in the Hf-rich area and can not be determined without further investigation.

It is worth to note that the composition of Region A is different from that of Region B. The Ta content is a little higher and the Hf content is a little lower in Region A than in Region B (Fig. 4). The reason for this difference is probably that the cooling rate of Region B, which is farer away from the ablation center, is higher than that of Region A. Therefore, the content of high-melting-point component HfO_2 is higher in Region B, and the content of low-melting-point component Ta_2O_5 is higher in Region A.

No Zr-contained component was found, probably because the evaporating rate of ZrO_2 is one magnitude higher than HfO_2. This phenomenon indirectly indicates that the HfC-based composite has a better anti-ablation performance than ZrC-based does.

Fig. 5 shows the morphology of C/C preform after ablation at the same condition. The depth of the ablation pit is much larger than that of the C_f/HfC composite with a shape of taper hole. The carbon fibers were burnt out orderly by the laser. The linear ablation rate of several kinds of anti-ablation composites are compared in Table 2. The C_f/HfC composite prepared in present work represents the best anti-ablation performance, with the linear ablation rate of only 0.008mm/s. The reason for the excellent anti-ablation performance of C_f/HfC composite is discussed as follows.

First, a large amount of heat was taken away with the melt and evaporation of SiO_2, HfO_2, ZrO_2 and Ta_2O_5. Second, HfO_2, ZrO_2 and Ta_2O_5 in liquid state at the ablated temperature spread out and sealed the cracks and holes in the composite. Third, a Ta_2O_5•mHfO_2 melt with a low vapor pressure and high viscosity was formed, which would block the diffusion of the oxygen to the inner of the composite. Last, the melt of Ta_2O_5•mHfO_2 strongly reflected the laser and emitted drastic incandescent light as the ablation went on.

Materials	Linear ablation rate, mm/s
C/ZrB_2-SiC [10]	0.066
C/SiC-TaC[11]	0.038
C/SiC[11]	0.083
C/SiC-ZrB2-TaC[12]	0.026
C_f/HfC (present work)	0.008

Table 2. Comparison of linear ablation rates of different composites from peer's work

4 Conclusions

A C_f/HfC composite was obtained by reaction melt infiltration (RMI) using 50Hf10Zr40Si3Ta alloy and C/C preform at 1900℃. The composite exhibits excellent oxidation-resistant and ablation-resistant properties because of the behavior of various oxides formed during the ablation. However, longer tests are necessary for unequivocal definition of heat-protective characteristics of an offered material in the conditions of approached to the natural.

References

[1] Levine S.R., Opila E.J., Lorincz J.A., et al. UHTC Composites for Leading Edges. NASA Glenn Research Center. (2004)

[2] Levine S.R., Opila E.J., Halbig M.C., et al. Evaluation of ultra-high temperature ceramics for aeropropulsion use. *Journal of the European Ceramic Society*, **Vol.22**, pp. 2757-2768 (2002).

[3] Scatteia L., Riccio A., Rufolo G., et al. PRORA-USV SHS: Ultra High Temperature Ceramic Materials for Sharp Hot Structures. *AIAA*. (2005)

[4] Schwab S. T., Stewart C. A., Dudeck K. W., et al. Polymeric precursors to refractory metal borides. *Journal of materials science*, **Vol. 39**, pp. 6051-6055 (2004).

[5] Ohlhorst C.W., Vaughn W. L. Arc jet results on candidate high temperature coatings for NASA's NGLT refractory composite leading edge task [R]. NASA /Langley Research Center (2003).

[6] He H.W., Zhou K.C., Xiong X., et al. Investigation on decomposition mechanism of tantalum ethylate precursor during formation of TaC on C/C composite material [J]. *Materials Letters*. **vol.60**, pp3409-3412 (2006).

[7] Krenkel W. Cost effective processing of CMC composites by melt infiltration (LSI-process).*Ceramic enginering and science proceeding*, **Vol. 22**, pp. 443-454 (2001).

[8] Jayaseelan D.D., Rafael Guimarães de Sá, Brown P. Reactive infiltration processing (RIP) of ultra high temperature ceramics (UHTC) into porous C/C composite tubes. *Journal of the European Ceramic Society*,**Vol. 31**, pp. 361-368 (2011).

[9] Ye Y.C., Zhang H., Zhu L. A., Tong Y.G., Chen K., Bai S.X. *Preparation of C_f/HfC composites by instantaneous liquid in-filtration at low temperature based on alloy design and its ablation property* in "Proceeding of *2nd International Conference on Advanced Composite Materials and Technologies for Aerospace Applications*, Wrexham, England, (2012).

[10] Wang Y.G., Liu W., Cheng L.F., Zhang L.T. Preparation and properties of 2D C/ZrB_2–SiC ultra high temperature ceramic composites, *Materials Science and Engineering A*, **vol. 524**, pp. 129–133 (2009).

[11] Wang Y., Xu Y.D., Wang Y.G., Cheng L.F., Zhang L.T. Effects of TaC addition on the ablation resistance of C/SiC, *Materials Letters*. **vol.64**, pp. 2068-2071 (2010).

[12] Li L.L., Wang Y.G., Cheng L.F., Zhang L.T. Preparation and properties of 2D C/SiC-ZrB_2-TaC composites. *Ceramics International*, **vol.37**, pp. 891–896 (2011).